Chapter 7
Behavior of Composite Laminates with Drilled and Moulded Hole Under Tensile Load

7.1 Introduction

Nowadays, composite materials are used within primary load carrying aircraft structures. Recent examples are Boeing 787 and Airbus A350XWB where the composite weight content has increased to 50–60 % [22]. However, joining of a composite part on a structure often requires manufacturing holes in order to place bolts or rivets. To obtain these holes, different processes can be implemented such as drilling or moulding. Drilling process concerns a conventional machining procedure where the composite materials are machined to produce hole. Nonetheless, it implies destruction of fibre continuity, large stress concentration and delamination at the hole entry and the hole exit [16, 7, 32]. Such result of damages can cause significant reduction in both tensile and compressive strength of composite structure [26, 27].

The destruction of the fibre continuity leads to the damage on the surface wall of the hole. According to the works of [32, 2, 30], this damage is affected by the interaction between the principal cutting edges of the drill and fibres orientation of the material machined. The results indicate that the machining quality of the wall of the hole is affected partly by the choice of cutting depth (feed rate of the tool) and the angle (θ) measured between the direction of fibres and the direction of cutting speed. For values of θ between $-45°$ and 90°, important damages are observed. These damages are mainly related to the rupture of fibres that is made by bending and shearing of the fibres of the composite part.

Several works have been published on the analysis of delamination at the entry and the exit of the hole. A number of works show that this damage is influenced by the choice of the machining parameters, the geometry of the cutting tool tip, and the nature of its material. All these authors are in agreement for that, the delamination located at the hole exit is caused mainly by the thrust force of the drill [1, 6, 8–11, 17, 18, 24, 29, 33]. For that various authors have been interested to the prediction of the thrust force analytically and numerically. The first analytical model based on the linear fracture mechanics is proposed by Hocheng and Dharan [14]. A 3D finite element analysis, based on fracture mechanics allowing to predict

V. Krishnaraj et al., *Drilling of Polymer-Matrix Composites*,
SpringerBriefs in Manufacturing and Surface Engineering,
DOI: 10.1007/978-3-642-38345-8_7, © The Author(s) 2013

the critical thrust force (for a two lip twist drill) responsible for this damage have been developed. In this modelling, the drill point geometry, the thrust force produced by the main cutting edges and the thrust force generated by the web of the drill are taken into account. The critical thrust forces obtained using this model is compared with those given by the analytical models developed by Hocheng [14]. The results show that the analytical model underestimates the critical thrust forces. Another numerical model has been developed by Zitoune [34]. This modelling is based on the damage mechanics with consideration for the various criteria for damage initiation.

As discussed by Torres et al. [27], conventional drilling leads to a reduction on the mechanical properties of composites structures. This reduction can be quantified by Residual Strength Diagrams which plot the strength of structure as a function of the hole diameter. They found that strength can be represented as an exponential function of hole's size and the orthotropic strength factor which involves the material properties. On the other hand, moulding consists of placing a pointed steel punch to spread out the fibres during the composite lay-up with an aim to leave a hole after polymerization. This process distributes locally the fibre placement at the edge of the hole.

The stress field around the hole in a composite plate under tension has been widely studied in the literature. Several analytical criteria for drilled and notched composites have been developed to predict failure modes. The principal assumption is that there is a stress concentration in damage vicinity which is a function of the material properties, specimen geometry and service loads. However, many of these criteria idealize the model by simplifying the material and geometry heterogeneities that can be observed near the edge of the hole. One of the most used failure criterion for drilled composites is the Point Stress Criterion (PSC) proposed in [25, 31]. This criterion defines a zone of stress intensification in the hole's surroundings as a function of the hole's radius. A similar approach was published by Tercan 2007 to determine the critical crack length at the edge of the hole. Additionally, a modification of PSC, called PWG and published in [5, 23], which assumes an exponential sensitivity of stress when a hole exists. With the same basis, the Damage Zone Criterion (DZC), which involves a maximum stress region around the hole was proposed by [12]. For non-local criterion, an approach called Fracture Characteristic Volume (FCV) was developed to take into account the stress gradient effect on the fracture of the composite laminate [13]. All these criteria and other several fracture models for composites with circular holes and cracks have been reviewed [4] to establish the more influent variables for this problem. Finally, the experimental technique of interferometry was applied by Toubal et al. [28] to determine the strain field and the stress concentration in woven fabric composites with circular hole under a longitudinal tensile load.

Few works concern specimens with moulded holes made of woven fabric, moreover, no literature is available on specimens made of unidirectional carbon fibres. Although the moulded holes require a specific mould for manufacture, the final outcome is comparable to the solution with drilled holes, and the cost of the

mould can be amortised over a period of time. Experimental works were carried out by Ng et al. [21], Lin et al. [20], Lin and Tsai [19], Hufenbach et al. [15] on the behaviour of composite panels and assembly with moulded hole under tensile load. In these studies a numerical procedure is used to predict the notched strength of the specimens with moulded hole. The results showed a strength dependency to the hole's diameter. For the same hole size, the predicted failure strength of specimens with moulded holes using numerical analysis have a higher value which are slightly higher than the experimental ones. On the other hand, the experimental study proposed by [20] leads to larger failure strength, smaller the initial stiffness and larger the failure strain of [0°/90°]s laminates with a moulded hole compared to those with a drilled hole. Lin et al. [19] uses experimental and numerical methods to study the failure of bolted joints of glass woven composites with drilled and moulded holes. Failure tests are conducted with the sequence [0°/90°]s and [±45°]s of woven glass/polyester roving specimens with different hole sizes and ratios E/D (distance from the hole centre to the edge on the hole diameter). For E/D = 1, the results exhibit the fracture strength of the moulded specimens of about 30–50 % higher than those with drilled specimens. The same order of magnitude between them exits when the ratio is E/D > 2.

In this section, a comparison between two categories of perforated specimens loaded in tension has been presented. The holes of the first category are obtained by drilling and by moulding for the second category. The studied specimens are quasi isotropic made of unidirectional prepreg materials. In order to analyze the behaviour of the specimens in the vicinity of the hole, the strain field measurement with the three-dimensional Digital Image Correlation (DIC) technique is carried out. The results obtained with 3D DIC technique are compared with the strain gauge measurements. The pictures obtained by a CCD-camera are used to describe the damage mechanisms of the plates with drilled and moulded holes. In order to understand better the causes of damages produced near the moulded holes during the tensile tests, the void content and fibre content has been quantified using normalized and no normalized methods (image processing).

7.2 Experimental Procedure

Unidirectional prepregs of 0.25 mm made of carbon/epoxy composite are used for preparing CFRP specimen. The raw materials of laminated structures are provided by Hexcel composites and are referenced as UD HexPly® T300-M10 with 56 % fibre content. The Table 7.1 presents the mechanical properties of the UD CFRP prepreg obtained following the mechanical standard ASN-A 4102. The stacking sequence of the composite parts is quasi-isotropic. The UD prepreg used for manufacturing is contained between two rigid moulds. On these two rigid moulds, holes were machined and fitted with pointed steel punch which has been used to spread the fibres during the manufacture process of the composite plate and getting

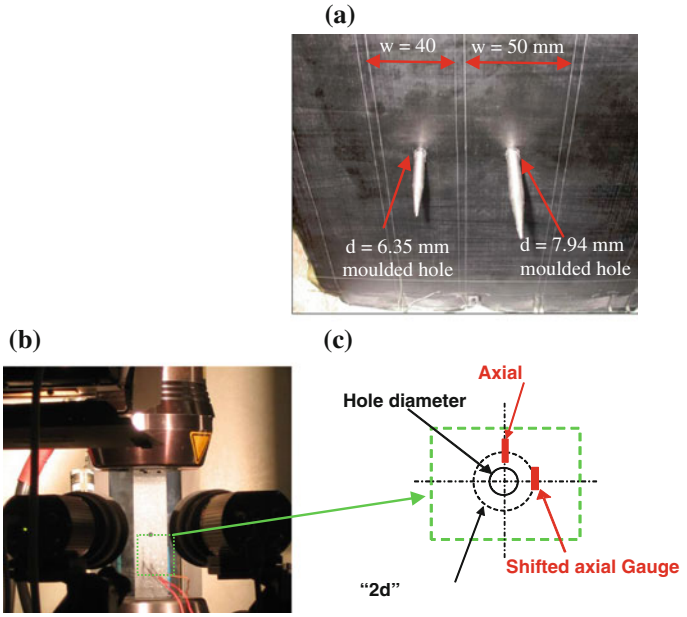

Fig. 7.1 Specimens for the tensile tests related to **a** mother plate from the mould, **b** Experimental device with DIC, **c** Scheme of the gauges position

Table 7.1 Mechanical properties of (T300/M10) carbon/epoxy unidirectional composites

Young's modulus (GPa)	Shear modulus (GPa)	Compressive modulus (GPa)	Poisson's ratio
$E_{11} = 125$, $E_{22} = 7$	$G_{12} = 3.2$	115	$\nu_{12} = 0.3$, $\nu_{21} = 0.016$, $\nu_{13} = 0.3$
Tensile strength (MPa)	In plane sheat strength (MPa)	Compressive strength (MPa)	Fiber content (%)
$\sigma_{11} = 1{,}600$ $\sigma_{22} = 80$	$\tau_{12} = 90$	1,400	56

a circular space after polymerization (Fig. 7.1a). The displacement of the pointed steel are activate when the resin reach the viscous phase. Vacuum and pressure are applied and maintained during the period of solidification.

In order to reduce the variability due to the manufacturing process all the specimens tested are obtained from the same mother plate. Two sets of specimens were tested (Fig. 7.1a). The first set concerns the specimens with moulded holes with diameter values of 6.35 and 7.94 mm. The second set includes the drilled hole specimens with the diameter values of the moulded holes. The diameter values used in this study are usually employed in the aeronautical field. For all specimens tested

the ratio between the hole diameter and the part width (d/w) is equal to 0.15 mm (Fig. 7.1a). The drilling is performed with a tungsten carbide drill (Twist drill).

A randomly distributed pattern is painted on the surface of the specimen for the strain field measurements thanks to Digital Image Correlation (DIC) technique (Fig. 7.1b). Moreover, on the same surface, two strain gauges (Fig. 7.1c) are pasted in the loading axis and located at a distance D (hole diameter) from the hole, which allows the axial strain measurement at two different places. Tensile tests were performed by means of an (Instron) UTM with a load capacity of 100 kN (Fig. 7.1b) at a speed of (2 mm/min). In order to better understand the different damage modes observed between drilled and moulded holes, the void content and fibre content analysis have been carried out using two methods. The first is normalized ASTM D3171 based on the dissolution of the specimen in sulphuric acid [3]. The second method is based on the image processing technique.

In order to quantify the variability of the void content as well as the fibre content in the vicinity of the moulded hole inducted by the manufacturing process, because of the need of the local information, here it is proposed the use of a method based on the technique of image processing. With the normalized method a mean value can be measured relative to the analysed material volume.

The technique of image processing principle consist of taking several SEM pictures of the plan "Pi" (i = number of plan). For this, specimens must firstly be prepared by polishing (See Fig. 7.2). Thanks to image processing the fibre content and the void content can be calculated statistically. In the SEM picture, voids, fibres and resin appear at different colours: white for fibres, grey for resin and black marks for voids. Using image processing software, it is simple to make only voids appear. The main idea here is to modify pictures in a binary form, which in fibres and matrix are associated with a white colour, and voids with black. In practice, it consists in setting a threshold to dissociate voids from the rest of the picture. Using this technique, voids surface content is equal to the ratio between black surface and the whole surface of the picture. The same principle is used to obtain the fibre ratio from all coupons.

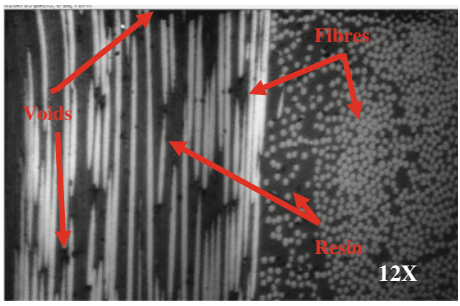

Fig. 7.2 SEM observation of the specimen thickness with 12X magnification

7.3 Results

7.3.1 Behaviour Analysis

Figure 7.3a shows the evolution of load versus measurements by the axial gauge for the drilled and moulded hole specimens with a 7.94 mm diameter (D). Failure strength for moulded hole is 30 % higher than the drilled hole. In addition, the axial gauge allows a local rigidity detection of the material in the moulded hole specimen which is smaller than the one detected on the drilled plate. After a detailed analysis, presence of a resin rich zone in the vicinity of the axial gauge is detected. The presence of the resin rich zone is related to the manufacturing process of the specimen with moulded hole which spreads the fibre around the hole. This analysis is verified by the X-Ray images obtained from specimens with moulded holes manufactured from textile structure [15].

Load versus strain curves given by the shifted axial gauge revealed that the local rigidity for moulded holes is higher than that of drilled holes (Fig. 7.3b). This difference can be explained by the fact that, in the area where the shifted axial gauges are pasted, the fibres are higher because of the stretched fibres o produce moulded hole. All the tested plates present the same results as presented in Fig. 7.3. Table 7.2 lists the average values of the failure strength for different studied specimens. It is found that the moulded hole specimens have higher residual strength compared with the drilled hole specimens. This gain is around 33 % for all specimens tested with 6.34 and 7.94 mm diameters.

The strain field, measured using the DIC technique, is confronted with strain gauges data. For the drilled hole, it is observed a good agreement between the two measuring techniques, with the maximum difference being about 5 %. With regard to the moulded hole specimens, the strain measurements are in good agreement with those obtained by the strain gauges when the applied load is lower than 28 kN (Figs. 7.4, 7.5). When the load reached 28 kN, damaged zones on the surface of the specimen are observed. This damage can be observed by the delamination of

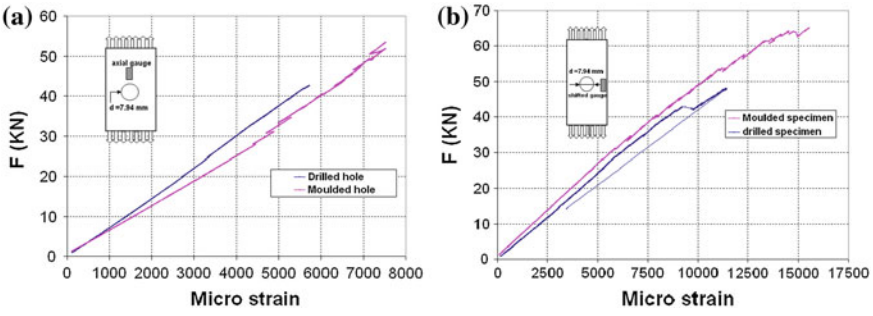

Fig. 7.3 Load versus gauges strains for specimens with moulded hole and drilled hole with 7.94 mm of diameter related to **a** axial gauge, **b** shifted axial gauge

Table 7.2 Average failure stress values for the different studied specimens

Diameters: d (mm)	Failure stress with drilled hole: σ (MPa)	Failure stress with moulded hole: σ (MPa)
6.34	349 ± 16	459 ± 35
7.93	386 ± 35	514 ± 40

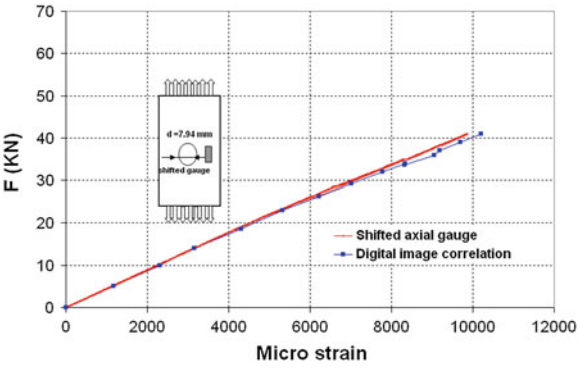

Fig. 7.4 Load versus strains, measurement comparison between DIC technique and strain shifted gauge related to drilled specimen with a 7.94 mm drill diameter

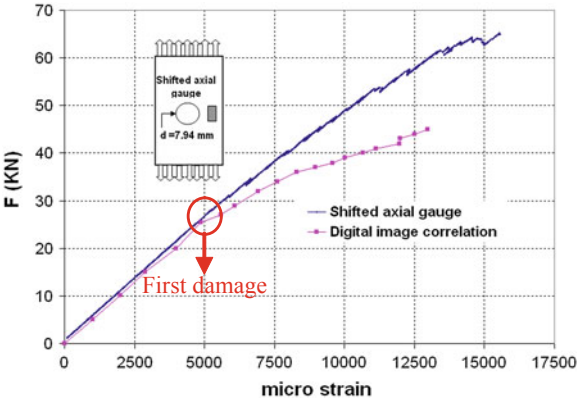

Fig. 7.5 Load versus strains, measurement comparison between DIC technique and strain shifted gauge related to moulded specimen with a 7.94 mm hole diameter

the above ply. This delamination affects the measurements taken, resulting into difficulties to achieve an accurate image correlation.

Image analysis provided by CCD camera shows a difference between the damage mode observed for the specimen with moulded hole and drilled hole for 7.94 mm diameter. Figure 7.5 shows a first damage occurrence for the specimen with moulded hole with the appearance of a crack oriented in the same direction as the 0° ply (or loading axis (OY)). This crack, observed at a given load value of 28 kN, is located at 1 mm at the edge of the hole (Fig. 7.6a). As the applied load increase, it is observed a second crack initiation (second damage) on the second edge of the moulded hole (at the right edge) and then a propagation of these two cracks in a parallel direction with regards to the fibre axis (Fig. 7.6a). With a load

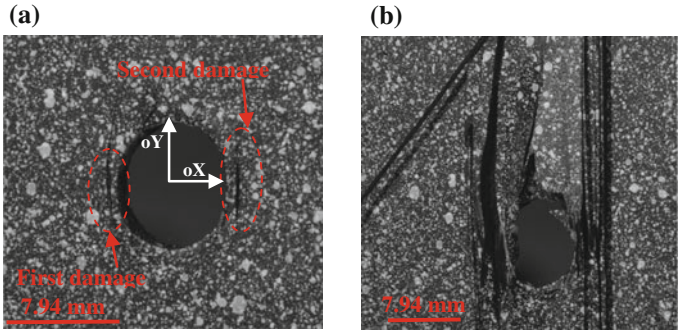

Fig. 7.6 Damage progression for different loading levels with 7.94 mm moulded hole related to **a** 47 kN loading, **b** 64 kN loading

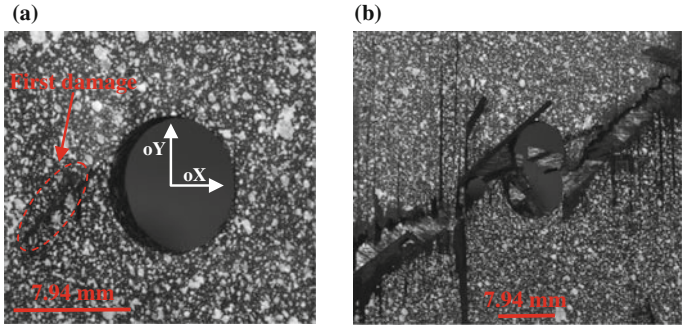

Fig. 7.7 Damage progression for different loading levels with 7.94 mm drilled hole related to **a** 42.5 kN loading, **b** 49 kN loading

value of 64 kN, the damage increase appears as a separation of the higher ply (Fig. 7.6b).

The CCD recorded sequences during the tensile test related to the drilled hole specimen show a different failure mode from that observed with a moulded hole. For a loading force lower than 42.5 kN, no damage is noticed. From 42.5 kN, a first damage (as a crack shape) oriented at 45° to the loading axis (OY) is observed (Fig. 7.7a). This crack remains stable until an amplitude of 48 kN (no propagation is observed). Moreover, when the loading reached 49 kN, a sudden failure of specimen is noted (Fig. 7.7b). All tested specimens present the same failure mechanisms. This mode of damage is similar to the drilled plates under tensile load [26].

It is noticed that, the damage mode versus the applied load for our moulded holes specimens (quasi-isotropic stacking sequence) made of UD prepreg is different compared to drilled holes, similarly the damaged are different for the moulded holes using woven fabrics with the same stacking sequence [21, 20, 15].

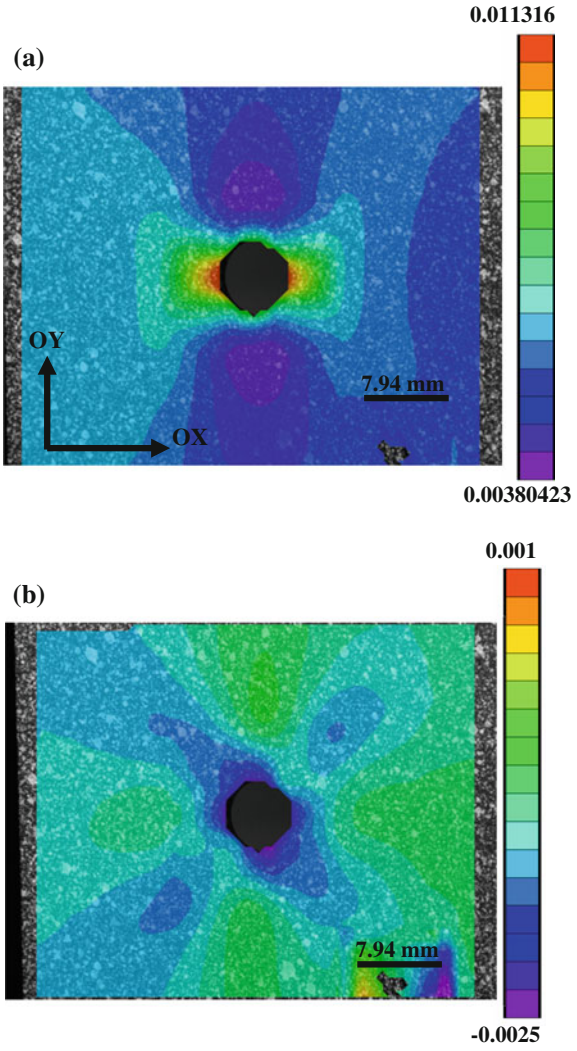

Fig. 7.8 Strain field distribution by the DIC technique for a 7.94 mm drilled hole specimen and a 25 kN loading amplitude related to **a** strain along the OY axis (ε_{yy}), **b** strain along the OX axis (ε_{xx}) (correlation carried out with 33-pixel of ZOI)

This difference can be explained due to the fibres trajectory near the hole as well as the amount of void content and fibre content in the vicinity of the hole.

Figure 7.8 shows the strain field distribution on the surface of a drilled hole specimen for a loading amplitude corresponding to 25 kN. These images are obtained with a 33-pixel size. In Fig. 7.8a, it is observed a positive strain along (OY) axis everywhere and a maximum value located at the edge of hole. For the strain field cartography along the transverse axis (OX), we notice the negative measured values (Fig. 7.8b). These strain results are caused by the Poisson modulus effect. However, for the same loading level, the strain amplitudes recorded on a drilled hole specimen are higher compared with those recorded on

moulded hole specimens (Figs. 7.8, 7.9). For a load of 25 kN, the axial strain ε_{yy} measured by the DIC for a plate with drilled hole is around 11,356 μdef. For the same test conditions and similar correlation parameters (DIC), the strain measured on specimen with moulded hole is around 6,000 μdef. For moulded holes, the fibre content is more important in the vicinity of the hole. This discrepancy can be linked to the difference in the local mechanical proprieties.

With the test conditions of the DIC image analysis carried out on the moulded hole specimens presented on the Fig. 7.9 (ZOI of 33 pixels), it is noticed that the transverse strain (along OX axis) presents a negative sign on all the structure. However, the crack opening phenomenon is observed around the hole thanks to the images provided by CCD camera. It results into a stress field with a positive sign

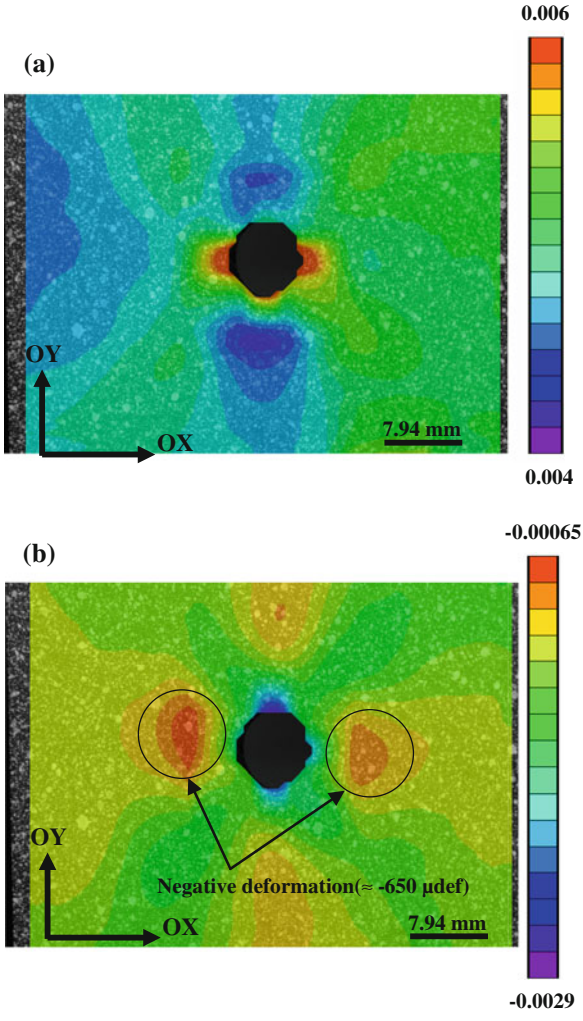

Fig. 7.9 Strain field distribution by the DIC technique for a 7.94 mm moulded hole specimen and a 25 kN loading amplitude related to **a** strain along the OY axis (ε_{yy}), **b** strain along the OX axis (ε_{xx}) (correlation carried out with 33-pixel of ZOI)

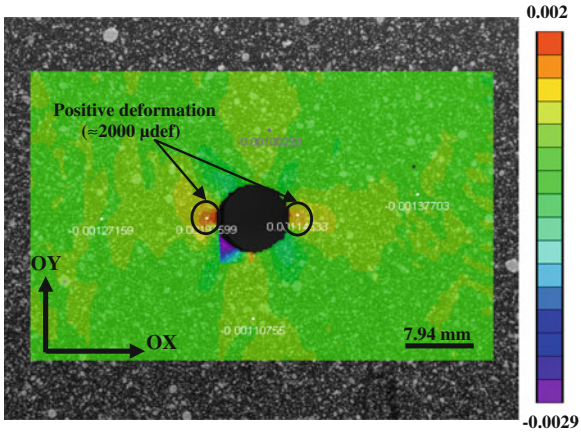

Fig. 7.10 Strain field distribution (ε_{xx}) by the DIC technique for a 7.94 mm moulded hole specimen and a 25 kN loading amplitude with the condition of correlation of 19 pixel of ZOI

along the OX axis. For this reason, additional correlation is carried out by means of a 19 pixels numerical gauge (ZOI). With this conditions, the result shows that, on one hand a positive transverse strain (along OX axis) near the hole is measured and it is in agreement with the opening crack phenomenon observed during the tensile test (Fig. 7.10); on the other hand the physical information is lost and this can be induced by the measurement noise or the quality of the specimens random pattern.

7.3.2 Fibre and Void Content Analysis Near the Moulded Hole

The use of the normalized method and no normalized method on five specimens cut far from holes give almost identical results. In this case, the mean values are respectively 4 and 56 % for the void content and the fibres content. The values of relative deviation are 0.5 % for the void content and 1 % for the fibres content. It can be assumed that this non-standardized method gives accurate results.

As shown in Figs. 7.11, 7.12, the results of this optical technique are presented for four positions (5, 6, 9 and 10) located respectively at 11.5, 9, 3.7 and 1.2 mm from the moulded hole centre in the Ox direction. From the Fig. 7.11 there is a small increasing of the fibre content and the void content measured in the plane 6 compared to these measured in the plane 5. At this step, it can be noted here that fibre ratio increase when the measurement comes near the hole, in both x and y directions. The maximal fibre content found is 57 % and it is measured close to the

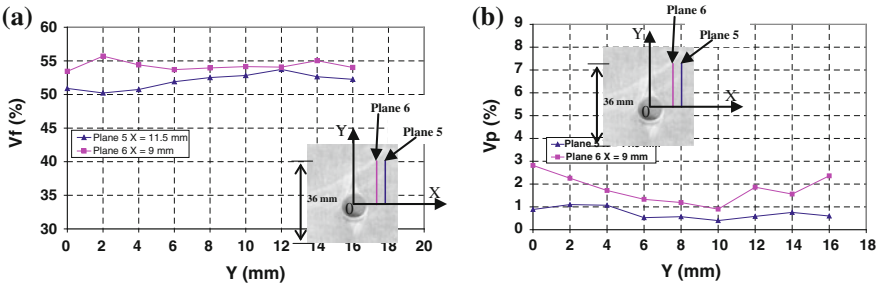

Fig. 7.11 Evolution of the fibre content and the void content along the loading direction (oY) in plane 5 and 6, **a** fibre content, **b** void content. Moulded plate with diameter of 6.35 mm

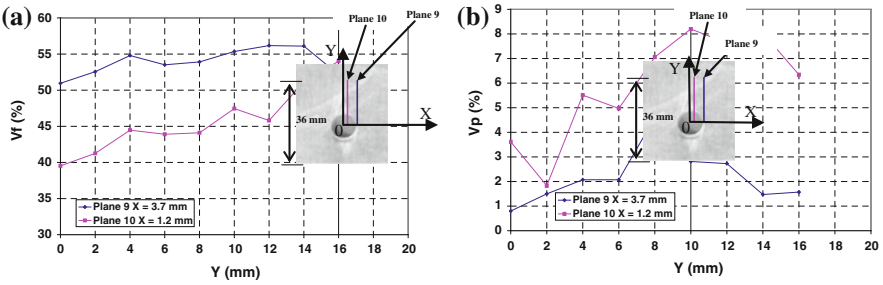

Fig. 7.12 Evolution of the fibre content and the void content along the loading direction (oY) in plane 9 and 10, **a** fibre content, **b** void content. Moulded plate with diameter of 6.35 mm

hole. At this location, picture analysis show that voids content is about 7 %. Modifications of void and fibre content can explain the onset of cracks during loading and fibre spread due to a lake of matrix.

7.4 Summary

This paper presents experimental results of drilled holes and moulded holes of composite specimens with quasi-isotropic stacking sequence made from UD prepreg and subjected to tensile loading. Based on the experimental analysis, the following conclusions were drawn.

1. The fracture strength for moulded hole specimens is higher than those obtained for drilled hole specimens. This difference is greater than 30 %. Although the fibre content around the moulded hole is higher than the drilled hole, it has been noted from strain gauge data that the local rigidity in tension for drilled specimens is higher than moulded specimens.

2. Moreover, the digital images obtained by the CCD Camera show different damage mechanisms between drilled holes and moulded holes specimens. For a plate with drilled hole, a sudden fracture is noticed and for the plate with moulded hole a progressive fracture is observed.
3. The strain fields measured by the DIC have shown that the maximum deformation (εyy) of drilled hole is twice higher compared to those of moulded hole. Also, the strain field cartography obtained from the test data leads to the strain along the transverse direction (OX) influenced by the size of the numerical correlation gauge. All the results obtained with the numerical correlation gauge corresponding to the 19-pixel size are in good agreement with the damage mechanisms observed by means of the CCD Camera.
4. The difference of the mechanical behaviour observed as well as the difference of the damage mode illustrated between the specimens with drilled and moulded hole were explained by the local measurement of the fibres content and void content carried out by the optical technique. In the plates with moulded holes, the void content in the vicinity of the hole is 8 % higher compared the void content far the hole.

References

1. Antoniomaria DL, Alfonso P, Francesco V (1996) Tool wear in drilling thermoset and thermoplastic matrix composites. Eng Syst Des Anal 75:41–46
2. Arola D, Ramulu M, Wang H (1996) Chip formation in orthogonal trimming of graphite/epoxy composites. Compos Part A 27A:121–133
3. ASTM D3171-99 (2004) Standard test methods for constituent content of composite materials. ASTM Int
4. Awerbuch and Madhukar (1985) Notched strength of composite laminates, predictions and experiments. J Reinf Plast Compos
5. Baselga Arino S, Maza Frechin M (2006) Methods for modelling the ultimate strength of orthotropic plate with a central hole under uniaxial tension. J Mater Sci 41:4365–4372
6. Campos Rubio J, Abrao AM, Faria PE, Esteves Correia A, Paulo Davim J (2008) Effect of high speed in the drilling of glass fiber reinforced plastic: evaluation of the delamination factor. Int J Mach Tool Manuf 48:715–720
7. Davim JP, Pedro R (2003) Drilling carbon reinforced plastics manufactured by autoclave—experimental and statistical study. Mater Des 24:315–324
8. Davim JP, Reis P (2003) Study of delamination in drilling carbon fiber reinforced plastics (CFRP) using design experiments. Compos Struct 59(4):481–487
9. Dharan CKH, Won MS (2000) Machining parameters for an intelligent machining system for composite laminates. Int J Mach Tools Manuf 40:415–426
10. Durão LMP, De Moura MFSF, Marques AT (2008) Numerical prediction of delamination onset in carbon/epoxy composite drilling. Eng Fract Mech 75(9):2767–2778
11. Erik P, Ingvar E, Leif Z (1997) Effects of hole machining defects on strength and fatigue life of composite laminates. Compos A 31:141–151
12. Eriksson and Arronson "Strength of tensile loaded graphite/epoxy laminates containing cracks, open and filled holes. J Compos Mater
13. Hochard C, Lahellec N, Bordreuil C (2007) A ply scale non-local fibre rupture criterion for CFRP woven ply laminated structures. Compos Struct 80:321–326

14. Hocheng H, Dharan CKH (1990) Delamination during drilling in composite laminates. J Eng Ind 112:236–239
15. Hufenbach W, Adam F, Kupfer R (2010) A novel notching technique for bolted joints in textile-reinforced thermoplastic composites. 14th European conference on composite materials, Paper ID: 461. Budapest, Hungary. 7–10 June 2010
16. Koënig W, Wulf Ch, Grass H, Willerscheid H (1985) Machining of fibre reinforced plastics. Ann CIRP 345:37–47
17. Krishnaraj V (2006) Study of drilling tool geometry while machining of glass fibre reinforced plastic. Ph.D Dissertation, Anna University, Chennai
18. Langella A, Nele L, Maio A (2005) A torque and thrust prediction model for drilling of composite materials. Compos A 36:83–93
19. Lin JH, Tsai CC (1995) Failure analysis of bolted connections of composites with drilled and moulded-in hole. Compos Struct 30:159–168
20. Lin JH, Tsai CC, Shie JS (1995) Failure analysis of woven-fabric composites with moulded-in holes bolted connections of composites with drilled and moulded-in hole. Compos Sci Technol 55:231–239
21. Ng SP, Tse PC, Lau KJ (2001) Progressive failure analysis of 2/2 twill weave fabric composites with moulded-in circular hole. Compos: Part B 32:139–152
22. Nilsson S, Bredberg A, Asp LE Size effects on strength of notched CFRP laminates loaded in bending. In: Proceeding of ICCM 17
23. Pipes and Wetherhold (1979) Notched strength of composites materials. J Compos Mater EUA
24. Singh I, Bhatnagar N, Viswanath P (2008) Drilling of uni-directional glass fiber reinforced plastics—experimental and finite element study. J Mater Des 29:546–553
25. Tercan M, Asi O, Aktaş A (2007) Determination of the critical crack length of notched weft-knitted glass fiber variable width composite plates. Compos Struct 77:111–119
26. Torres M, Gonzalez JL, Hernandez H (2009) Residual strength and fracture path for drilled epoxy-glass composites. Adv Mater Res 65:89–96
27. Torres M, Gonzalez JL, Hernandez H (2009) Fracture behavior characterization of composite tubes with hole defects under tensile load. Suplemento de la Revista Latinoamericana de Metalurgia y Materiales S1(3):1183–1188
28. Toubal L, Karama M, Lorrain B (2005) Stress concentration in a circular hole in composite plate. Compos Struct 68:31–36
29. Tsao CC, Ho-Cheng H (2005) Effect of eccentricity of twist drill and candle drill on delamination in drilling of composite materials. Int J Mach Tools Manuf 45:125–130
30. Wang DH, Ramulu M, Arola D (1995) Orthogonal cutting mechanisms of graphite/epoxy composite, Part I unidirectional laminate. Int J Mach Tools 35(1):1623–1638
31. Whitney and Nuismer (1974) Stress fracture criteria for laminates composites containing stress concentrations. J Compos Mater
32. Zitoune R, Collombet F (2005) Experiment-calculation comparison of the cutting conditions representative of the long fibre composite drilling phase. Compos Sci Technol 65:455–466
33. Zitoune R, Collombet F (2007) Numerical prediction of the thrust force responsible of delamination during the drilling of the long-fiber composite structures. Compos A 38:858–866
34. Zitoune R, Collombet F, Piquet R, Lachaud F, Pasquet P (2005) Experiment-calculation comparison of the cutting conditions representative of the long fibre composite drilling phase. Compos Sci Technol 65:455–466